PROCEEDINGS OF SPIE

SPIEDigitalLibrary.org/conference-proceedings-of-spie

Synthesis of high-Tg hole-transporting polymers with different redox potentials and their performance in organic two-layer LEDs

Erika Bellmann, Sean E. Shaheen, Seth R. Marder, Bernard Kippelen, Robert H. Grubbs, et al.

Erika Bellmann, Sean E. Shaheen, Seth R. Marder, Bernard Kippelen, Robert H. Grubbs, Nasser Peyghambarian, "Synthesis of high-Tg hole-transporting polymers with different redox potentials and their performance in organic two-layer LEDs," Proc. SPIE 3476, Organic Light-Emitting Materials and Devices II, (16 December 1998); doi: 10.1117/12.332629

Event: SPIE's International Symposium on Optical Science, Engineering, and Instrumentation, 1998, San Diego, CA, United States

Synthesis of high-T_g hole-transporting polymers with different redox potentials and their performance in organic two-layer LEDs

Erika Bellmann[a], Sean E. Shaheen[b], Seth R. Marder[c], Bernard Kippelen[b], Robert H. Grubbs[a], Nasser Peyghambarian[b]

[a]Arnold and Mabel Beckman Laboratories of Chemical Synthesis, Division of Chemistry and Chemical Engineering, California Institute of Technology, Pasadena, CA 91125

[b]Optical Sciences Center, University of Arizona, Tucson, AZ 85721

[c]Beckman Institute and The Jet Propulsion Laboratory, California Institute of Technology, Pasadena, CA 91109

ABSTRACT

Organic hole transport materials are used in organic LEDs, where they substantially improve device performance if placed as a hole transport layer (HTL) between the anode and the electroluminescent layer (EL). Soluble polymeric hole transport materials with high glass transition temperatures are of particular interest, because they allow for efficient device fabrication through spin casting of the HTL, and high glass transition temperatures have been found to improve thermal and long-term stability of the device. The redox potential of the hole transport material determines the facility of charge injection at the anode/HTL and the HTL/EL interfaces, thus affecting the overall device efficiency. We have synthesized a series of soluble hole-transporting polymers with glass transition temperatures in the range of 130°C to 150°C. The synthetic method allows facile substitution of the hole transport functionality with electron-withdrawing and electron-donating groups, which permits tuning of the redox potential of the polymer. These polymers have been used as HTL in two-layer devices ITO/HTL/Alq/Mg. The maximum external quantum efficiency increases, if the redox potential is changed to facilitate reduction of the hole transport material at the HTL/EL interface. Electron-deficient derivatives show higher external quantum efficiencies. The device stability, however, follows the opposite trend.

Keywords: hole-transporting polymer, two-layer organic LED, redox potential, external quantum efficiency, glass transition temperature

Part of the SPIE Conference on Organic Light-Emitting Materials and Devices II
San Diego, California • July 1998
SPIE Vol. 3476 • 0277-786X/98/$10.00

1. INTRODUCTION

Organic LEDs are often two-layer devices, where a film of a hole-transporting material (HTL) is placed between the anode (most commonly ITO = indium tin oxide) and the electroluminescent layer (EL) (Figure 1). The hole-transporting material traps the electrons inside EL and promotes hole transport to the EL. This facilitates the exciton formation inside the EL or at the HTL/EL interface consequently improving the overall device characteristics. Most relevant for the device performance are the following three properties of the hole transport material: hole mobility within the material, its redox potential and its thermal/electrochemical stability.

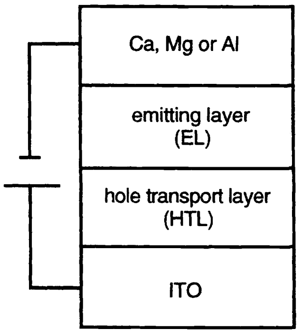

Figure 1: Schematic representation of a two-layer organic LED

Hole mobilities in organic materials have been widely studied[1-5] and have been correlated with device performance.[6] The redox potential determines how easily the material is oxidized at the ITO/HTL interface or how easily it is reduced at the HTL/EL interface. Relatively electron-rich compounds are commonly used as hole transport materials,[7] since facile hole injection at the ITO/HTL interface is expected to promote device function. Materials with a lower energetic barrier for hole injection into the HTL, however, have at the same time a higher barrier for reduction at the HTL/EL interface. It is therefore difficult to predict which redox behavior is optimal for the overall device performance. In this study we examine how the redox potential of the hole transport material affects the characteristics of a two-layer organic LED.

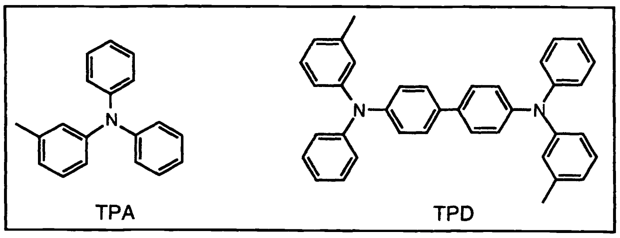

Figure 2: Structures of TPA and TPD

We report the synthesis of a series of analogous hole transport materials with systematic variation of the redox potential. The hole-transporting functionalities are derivatives of the well-studied organic hole-transporting molecules TPA and TPD[7] (Figure 2). The hole-transporting functionalities are covalently incorporated into a polymer. By preparing a high molecular weight hole-transporting material we attempt to achieve desirable film formation properties and high glass transition temperatures.

2. PREPARATION OF THE MATERIALS

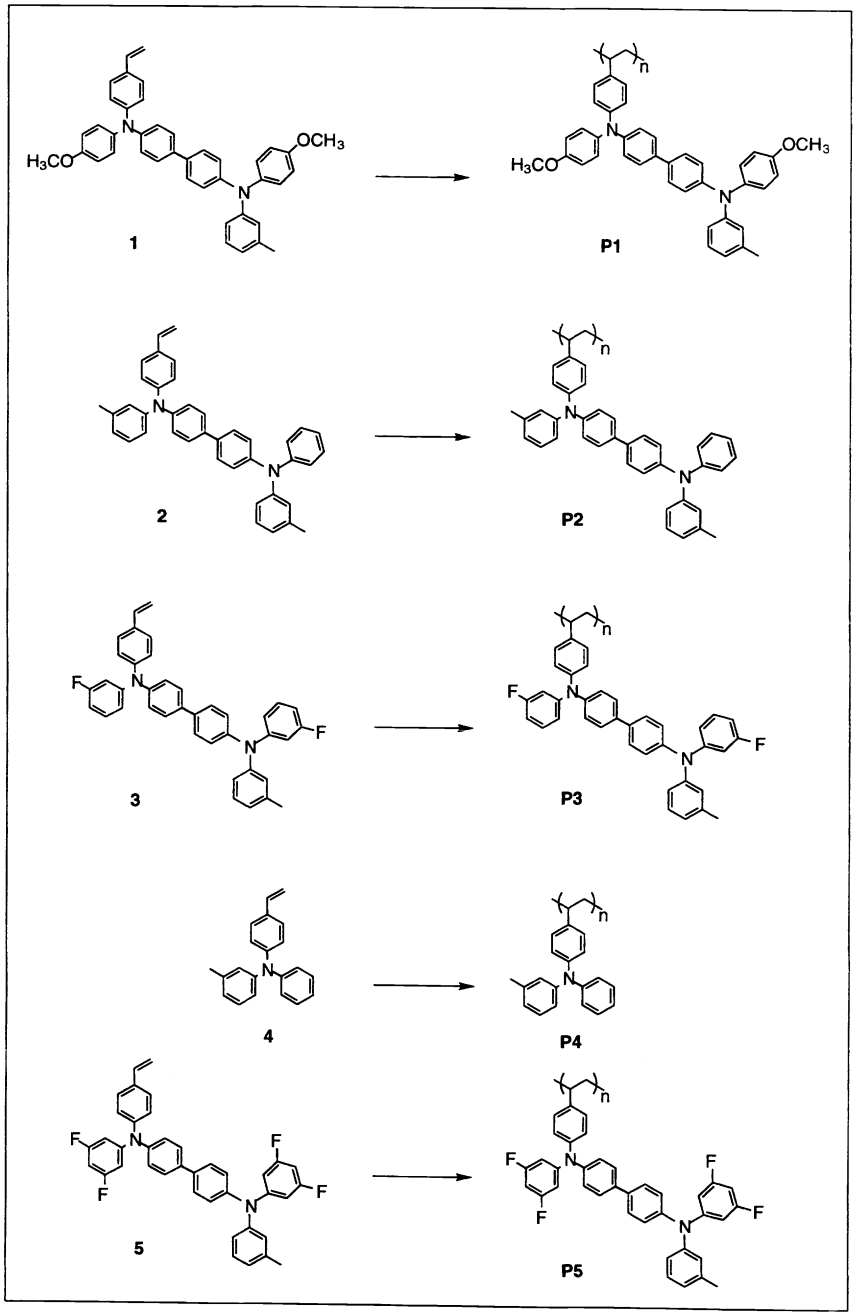

Figure 3: Structures of the synthesized hole-transporting polymers and the corresponding monomers

Previous studies suggest that polymers with non-polar compact backbones exhibit higher hole mobilities and show improved performance as hole transport layers in LEDs.[1-6] Therefore, the monomers were designed to contain a styrene type functionality, which would permit anionic polymerization resulting in an all-hydrocarbon compact backbone (Figure 3). Electron-donating and electron-withdrawing substituents were introduced to provide for different redox potentials. The differences in hole mobilities between the polymers **P1-P5**, however, are presumed to be minimal since the hole-transporting functionalities have a similar structure and their environment (e.g. backbone of polymer) is identical.[1]

We have prepared different monovinylated TPD derivatives by an efficient three-step procedure based on Palladium-catalyzed amination[8-11] (Scheme 1). This method allows independent choice of the substituent patterns of the outer phenyl rings. Therefore, in addition to the derivatives presented here a large variety of asymmetrically substituted TPDs can be prepared using this methodology. The TPA monomer **4** was synthesized in a similar fashion (Scheme 1).

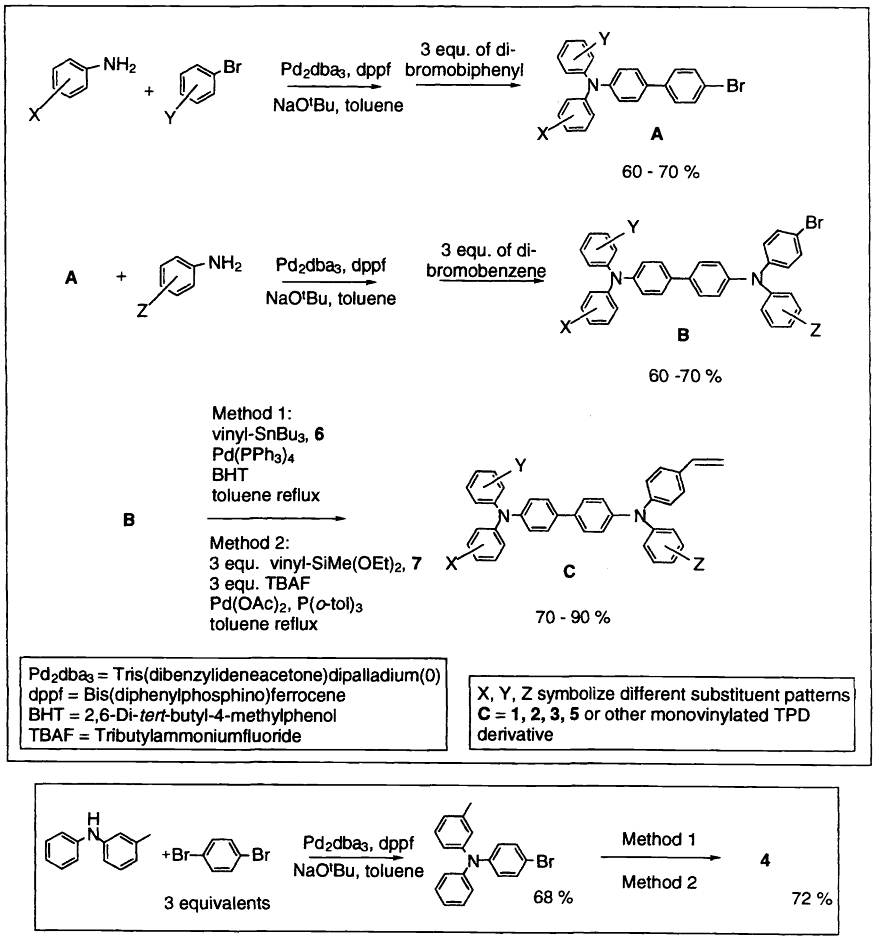

Pd_2dba_3 = Tris(dibenzylideneacetone)dipalladium(0)
dppf = Bis(diphenylphosphino)ferrocene
BHT = 2,6-Di-*tert*-butyl-4-methylphenol
TBAF = Tributylammoniumfluoride

X, Y, Z symbolize different substituent patterns
C = **1, 2, 3, 5** or other monovinylated TPD derivative

Scheme 1: General synthetic procedure for asymmetrically substituted monovinyl-TPDs and synthesis of monovinyl-TPA

In the last step of the monomer synthesis, the monovinyl compounds **C** are obtained by Palladium-catalyzed vinylation. The desired products were prepared in high yield using the tin reagent **6** or an excess of the silicon reagent **7** (Scheme 1). Nickel-catalyzed reaction of the bromoderivatives **B** with vinyl-Grignard[12-13] did not result in formation of the desired product. An other synthetic route involves substitution of the bromine in **B** by –CHO via lithiation and quenching with dimethylformamide and reaction of the aldehyde with the appropriate Wittig reagent or the appropriate Titanium reagent[14] to form the vinyl group. The transformation of **B** to **C** via the aldehyde, however, was associated with considerably lower yields (around 40%) of the monovinyl product.

The anionic polymerization of **1-4** was initiated by 0.05 equivalents of *n*-butyllithium (*n*-BuLi) at -78°C. In case of the monomer **5** the two Fluorine substituents in the 3- and 5-position of the outer phenyl rings cause the aromatic Hydrogen in between them to be reactive towards strong bases. *n*-BuLi was observed to deprotonate the TPD core prior to initiating polymerization. The polymerization of the dianion was possible in a dilute THF solution and yielded the target polymer after quenching with methanol at -78°C. Side reactions of the dianion species caused part of the material to crosslink during polymerization. The insoluble crosslinked fraction was removed by filtration. The isolated yield of the polymer **P5** is therefore significantly lower than the yields of the polymers **P1-P4.**

All of the resulting polymers show high glass transition temperatures, are thermally stable up to 400 °C, are soluble and form high quality transparent thin films upon spin casting. The solutions and the films display blue fluorescence. The polymer properties are summarized in Table 1.

Table 1: Polymerization results and conditions

polymer	polymerization conditions	isolated yield [%]	M_W[a]	PDI[a]	T_g [°C]	T_{TGA}[b] [°C]
P1	toluene/THF=10/1, -78°C, 0.05 equ. *n*-BuLi	96	15700	1.28	132	408
P2	toluene/THF=10/1, -78°C, 0.05 equ. *n*-BuLi	98	11150	1.13	151	400
P3	toluene/THF=10/1, -78°C, 0.05 equ. *n*-BuLi	98	11500	1.16	147	414
P4	toluene/THF=10/1, -78°C, 0.05 equ. *n*-BuLi	96	5000	1.09	104	397
P5	THF, -78°C, 2.05 equ. *n*-BuLi	65	6550	1.30	140	412

[a] determined by gel permeation chromatography in methylene chloride versus monodispersed polystyrene standards

[b] temperature of thermal decomposition determined by thermal gravimetric analysis and reported as temperature of onset of weight loss

3. CYCLIC VOLTAMMETRY

The redox potentials of the polymers have been determined by cyclic voltammetry in methylene chloride versus ferrocene/ferrocenium (Table 2). The redox potentials of the polymers **P1-P3** and **P5** are similar to the redox potentials of the corresponding molecular compounds[11] (Table 2), showing that incorporation into the polymer does not substantially alter the redox behavior of the hole-transporting functionality. The separation between the cyclic voltammetry peaks in forward and reverse bias for these polymers is approximately 59 mV and no change in the cyclic voltammetry curves is observed after 10 scans, suggesting that the redox potentials are reversible. The TPA based polymer **P4** shows an irreversible redox potential, which is lower than the redox potential of the molecular TPA. TPA is known to be less electrochemically stable than TPD derivatives.[15]

The polymer **P1** has the lowest redox potential. It is easiest to oxidize at the ITO/HTL interface but the energetic barrier at the HTL/EL interface is highest. The redox potential increases in the order **P1-P5**. In the case of **P5** the hole injection from ITO is least favored but the reduction at the HTL/EL interface occurs most readily.

The results of the solution measurements show the trends in redox behavior of the materials relative to one another. These trends are the same in an LED. The absolute values, however, can not be directly applied to the situation of a working device, since the redox processes in an LED occur from a solid state film. Photoelectron spectroscopy of the polymer films will be performed in the future and will provide additional information.

Table 2: Redox potentials of the HTL materials

polymer	^{1}E1/2 [mV]	^{2}E1/2 [mV]	redox potentials of the corresponding molecular compounds [mV]
P1	150	355	^{1}E1/2 = 160, ^{2}E1/2 = 400
P2	280	480	^{1}E1/2 = 260, ^{2}E1/2 = 510
P3	390	560	^{1}E1/2 = 360, ^{2}E1/2 = 580
P4	$^1E_p = 490^a$, $^2E_p = 380^a$ ("E1/2" = 435)^a		$^1E_p = 550^a$, $^2E_p = 470^a$
P5	490	590	^{1}E1/2 = 510, ^{2}E1/2 = 660

error of the measurement is estimated to ± 10 mV

^{a}irreversible redox potential

4. FABRICATION AND CHARACTERIZATION OF ORGANIC TWO-LAYER LEDs

Devices were fabricated on indium tin oxide (ITO) coated glass substrates with a sheet resistance of 20 ohms/sq (Donnelly Corporation) which had been ultrasonicated in acetone and methanol, dried in a stream of nitrogen, and then plasma etched for 60 seconds. Layers of the hole-transporting polymers (40 nm) were formed by spin casting from chlorobenzene solutions (10 g/L). The second layer consisted of vacuum vapor deposited tris(8-quinolinolato)aluminum (Alq) (50 nm), which had been purified by recrystallization and sublimation prior to deposition. Mg cathodes (200 nm) were thermally deposited at a rate of 8 Å/s through a shadow mask to create devices 3 x 5 mm in area. Current-voltage and light output characteristics of the devices were measured in forward bias. Device emission was measured using a silicon photodetector at a fixed distance from the sample (12 cm). The response of the detector had been calibrated using several test devices, for which the total power emitted in the forward direction was measured with a NIST traceable integrating sphere (Labsphere). Photometric units of cd/m^2 were calculated using the forward output power and the electroluminescence spectra of the devices. Efficiencies were measured in units of external quantum efficiency (% photons/electron). Cathode deposition and device characterization were performed in a nitrogen dry box (VAC).

Devices show typical Alq-emission[16] resulting in green LEDs. Table 3 and Figure 4 summarize the device data. The maximum external quantum efficiency increases substantially as the redox potential becomes more positive until an optimum value is reached (**P3**). Thus, this study suggests that higher quantum efficiencies will be achieved with hole-transporting materials which are more electron-deficient than the commonly used TPD. If the redox potential is increased further, the energetic barrier at the HTL/EL interface is further decreased but the barrier for hole injection into the HTL becomes too high. This causes the external quantum efficiency to decrease again (**P5**).

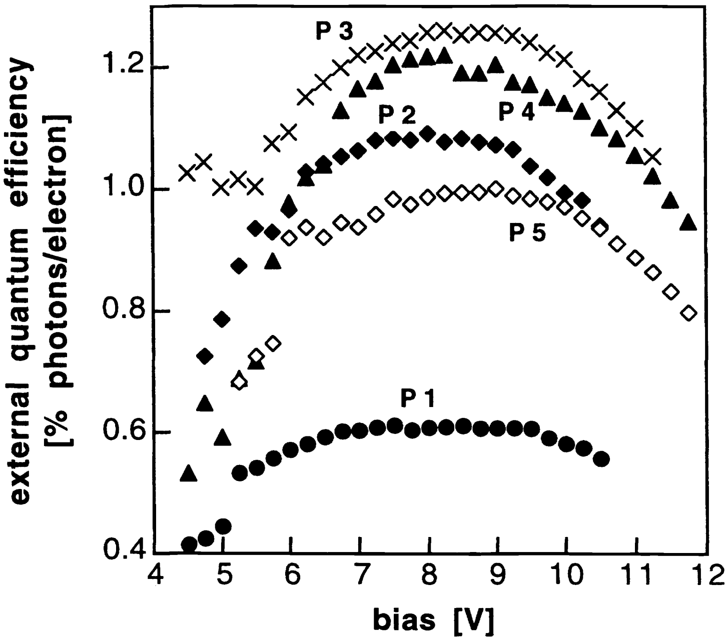

Figure 4: External quantum efficiency versus bias voltage for the devices ITO/HTL/Alq/Mg with polymers **P1** through **P5** as hole transport materials

Table 3: Device characteristics versus redox potential of the hole transport material for the devices ITO/HTL/Alq/Mg

HTL-polymer	$^1E1/2$ [mV]^a	operating voltage [V]^c	max. ext. quantum efficiency [% photons/e$^-$]	light output at 10 V [cd/m^2]
P 1	150	4.5	0.61	2300
P 2	280	4.75	1.09	2900
P 3	390	4.5	1.25	3700
P 4	435^b	4.5	1.22	1800
P 5	490	5.25	1.00	1000

[a] determined by cyclic voltammetry in methylene chloride solution versus ferrocene/ferrocenium

[b] please see Table 2: irreversible redox potential reported as $(^1E_p+^2E_p)/2$

[c] light output $\geq$ 5 cd/m^2

To test the stability of the devices, the LEDs have been operated at 6 mA constant current (corresponds to 50 mA/m^2) in a nitrogen dry box. The observed changes in external quantum efficiency are illustrated in Figure 5. The device with **P1** as hole-transporting material was the least efficient one at the beginning of the lifetime study but retained 60 % of it's initial efficiency after 1h of continuous operation. Devices which contained **P3, P4** and **P5** decomposed fast. After 1h the trend in performance was reversed with ITO/**P1**/Alq/Mg showing the highest external quantum efficiency at this time.

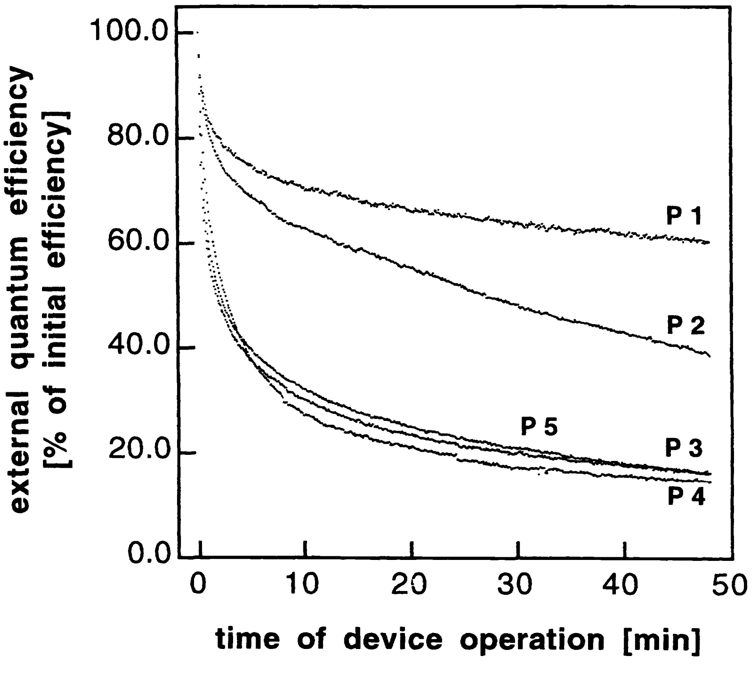

Figure 5: Lifetime study for the devices ITO/HTL/Alq/Mg

Since all the other device components were kept the same, this experiment shows the relative stability of the hole transport materials under device operation conditions. Possible decomposition pathways are thermal or photochemical degradation within the HTL or decomposition via a redox process at the ITO/HTL interface or the HTL/Alq interface. The observed degradation and trends in device stability can not be explained with thermal or photochemical processes within the HTL, since all of the studied materials have similar high thermal stabilities (Table 1) and do not absorb light above 410 nm. Most likely, the decomposition of the HTL is caused by redox reactions at the interfaces. The degradation process depends on the redox potential. Hole transport materials with a more positive redox potential yield devices with higher external quantum efficiencies but are more susceptible to degradation.

5. CONCLUSIONS

We have developed an efficient synthetic method for the preparation of a variety of soluble hole-transporting polymers with compact non-functionalized backbones and high glass transition temperatures. We have synthesized several hole transport materials with differences in their redox potential and we have investigated the effect of the redox potential on the performance of a two-layer LED.

This study shows that HTL materials which are easily oxidized yield devices with lower external quantum efficiencies. Devices containing HTL materials with a more positive redox potential exhibit higher external quantum efficiencies, suggesting that facile hole injection from the anode into the HTL is not crucial for the overall device performance. However, if the energetic barrier for hole injection at the anode/HTL interface is too high, it will have a negative impact on the device characteristics. Consequently, there is an optimum value for the redox potential. More specifically, we find that the redox behavior of unsubstituted TPD is not optimal. Higher quantum efficiencies have been observed for polymers containing TPA and difluoro-TPD (**P4** and **P3**).

Device stability was also found to depend on the redox potential of the HTL material. Derivatives with higher redox potentials yield devices with shorter lifetimes. Apparently, facile reduction of the HTL material not only promotes the desired charge transfer processes at the HTL/EL interface but also speeds up degradation reactions.

6. ACKNOWLEDGMENTS

We thank Prof. Neal R. Armstrong for very helpful discussions and Dr. Steven Barlow for valuable technical assistance with the cyclic voltammetry. Furthermore, we would like to thank Dr. Steven Barlow and Dr. S. Thayumanavan for providing samples of the molecular TPD derivatives. Financial support was received through the Center for Advanced Multifunctional Nonlinear Optical Polymers and Molecular Assemblies (CAMP) from the Office of Naval Research.

7. REFERENCES

(1) Bässler, H. *Phys. Status Solidi (b)* **1993**, *175*, 15 and references therein.

(2) Van der Auweraer, M.; De Schryver, F. C.; Borsenberger, P. M.; Fitzgerald, J. J. *J. Phys. Chem.* **1993**, *97*, 8808.

(3) Borsenberger, P. M.; Pautmeier, L.; Richert, R.; Bässler, H. *J. Chem. Phys.* **1991**, *94*, 8276.

(4) Gruenbaum, W. T.; Sorriero, L. J.; Borsenberger, P. M.; Zumbulyadis, N. *Jpn. J. Appl. Phys.* **1996**, *35*, 2714.

(5) Heun, S.; Borsenberger, P. M. *Physica B* **1995**, *216*, 43.

(6) Bellmann, E.; Shaheen, S. E.; Thayumanavan, S.; Barlow, S; Grubbs, R. H.; Marder, S. R.; Kippelen, B.; Peyghambarian, N. *Chem. Mater.* in press.

(7) Tsutsui, T. *MRS Bulletin* **June 1997**, 39 and references therein.

(8) Wolfe, J. P.; Rennels, R. A.; Buchwald, S. L. *Tetrahedron* **1996**, *52*, 7525.

(9) Wolfe, J. P.; Wagaw, S.; Buchwald, S. L. *J. Am. Chem. Soc.* **1996**, *118*, 7215.

(10) Driver, M. S.; Hartwig, J. F. *J. Am. Chem. Soc.* **1996**, *118*, 7217.

(11) Thayumanavan, S.; Barlow, S.; Marder, S. R. *Chem. Mater.* **1997**, *9*, 3231.

(12) Tamao, K.; Sumitani, K.; Kumada, M. *J. Am. Chem. Soc.* **1972**, *94*, 4374.

(13) Nugent, W. A.; McKinney, R. J. *J. Org. Chem.* **1985**, *50*, 5370.

(14) Pine, S. H. *Organic Reactions* **1993**, *43*, 1.

(15) Yano, M.; Furuichi, M.; Sato, K.; Shiomi, D.; Ichimura, A.; Abe, K.; Takui, T.; Itoh, K. *Synth. Met.* **1997**, *85*, 1665.

(16) Tang, C. W.; VanSlyke, S. A. Appl. Phys. Lett. **1987**, *51*, 913.